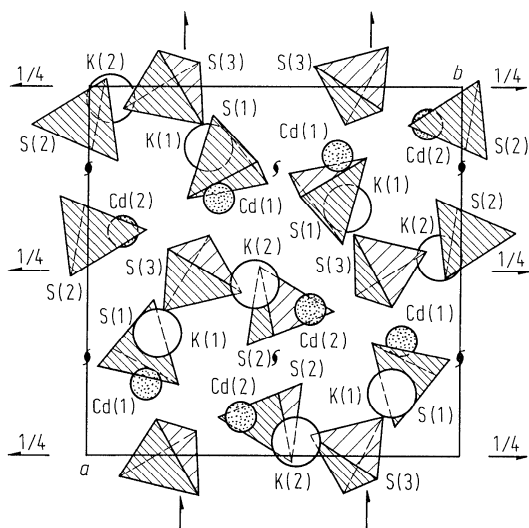
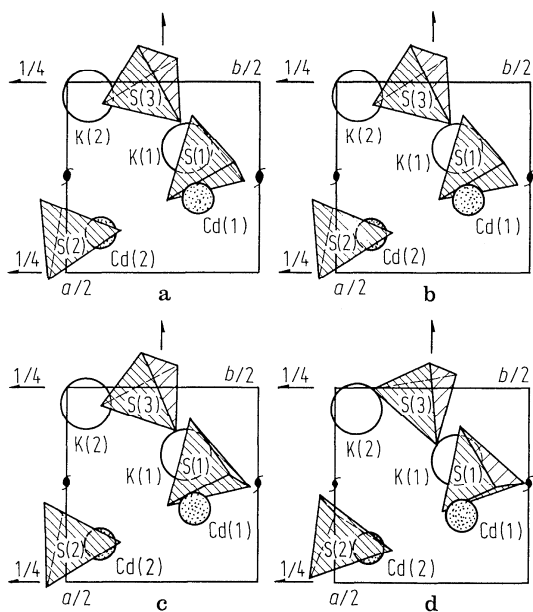


**Fig. 43A-12-001.**  $\text{K}_2\text{Cd}_2(\text{SO}_4)_3$ . Phase diagram of  $\text{CdSO}_4$ - $\text{K}_2\text{SO}_4$  system [77Nas].



**Fig. 43A-12-002.**  $\text{K}_2\text{Cd}_2(\text{SO}_4)_3$ . Crystal structure of phase II [77Abr]. Projection on (001).



**Fig. 43A-12-003.**  $K_2Cd_2(SO_4)_3$ . Crystal structure [78Abr]. Projection of asymmetric units on (001). (a) at 298 K, (b) at 390.5 K, (c) at 417.5 K, (d) at 443.5 K.

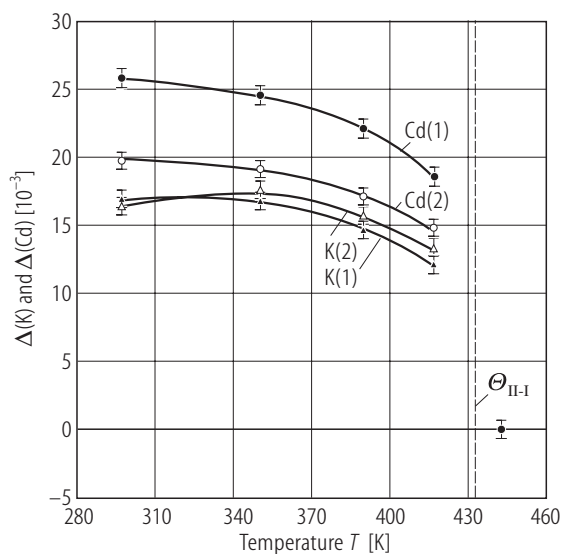
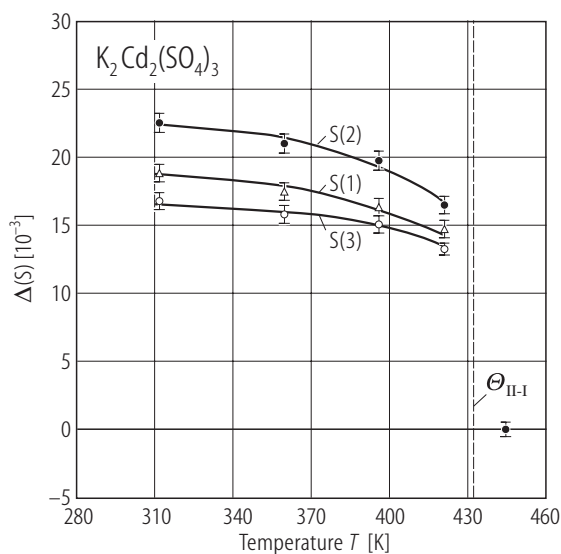


**Fig. 43A-12-004.**  $K_2Cd_2(SO_4)_3$ .  $\Delta(S)$ ,  $\Delta(K)$ ,  $\Delta(Cd)$  vs.  $T$  [78Abr].  $\Delta(S)$ : displacements of sulfur atoms from the cubic positions;  $\Delta(K)$  and  $\Delta(Cd)$ : displacements of K and Cd atoms from the [111] axis, in fractional coordinates. Average unit cell parameters are 10.219 Å at 298 K and 10.270 Å at 443.5 K.

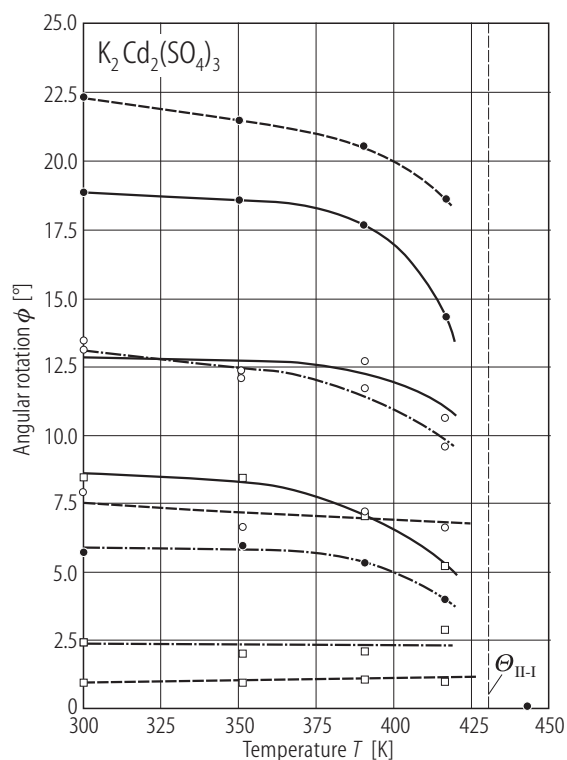


**Fig. 43A-12-005.**  $\text{K}_2\text{Cd}_2(\text{SO}_4)_3$ .  $\phi$  vs.  $T$  [79Lis].  $\phi$ : rotation angle of sulfate ion. The dashed, dot dashed and solid lines correspond to S(1), S(2) and S(3) sulfate ions, respectively. The dots, open circles and open squares distinguish the rotation angles about the two-fold rotation axes of each sulfate tetrahedron.

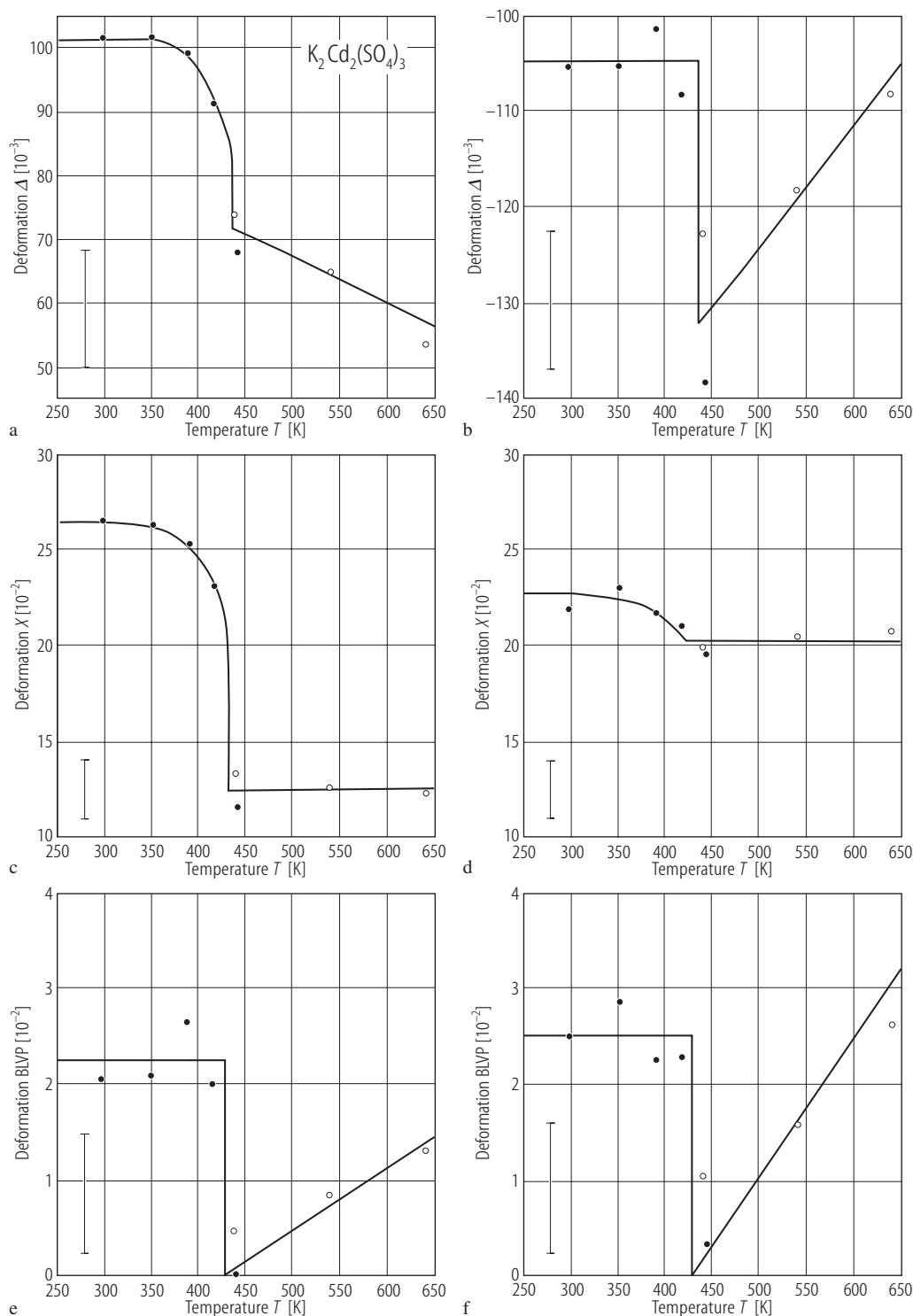


**Fig. 43A-12-006.**  $\text{K}_2\text{Cd}_2(\text{SO}_4)_3$  (2% Co doped).  $\Delta$ ,  $X$ , BLVP vs.  $T$  [89Per]. For definitions of  $\Delta$ ,  $X$ , see caption of Table 43A-12-005. BLVP (bond length variation parameter) is defined by  $(\overline{B_1} - \overline{B_2})/(\overline{B_1} + \overline{B_2})$ , where  $\overline{B_1}$  and  $\overline{B_2}$  are the averages of the three longest and the three shortest Cd-O bonds, respectively. (a), (c), (e) for  $\text{CdO}_6-1$ ; (b), (d), (f) for  $\text{CdO}_6-2$ .  $\text{CdO}_6-1$  and  $\text{CdO}_6-2$  are two kinds of different octahedra. Open circles: [89Per]. Full circles: results calculated using the data of [77Abr].

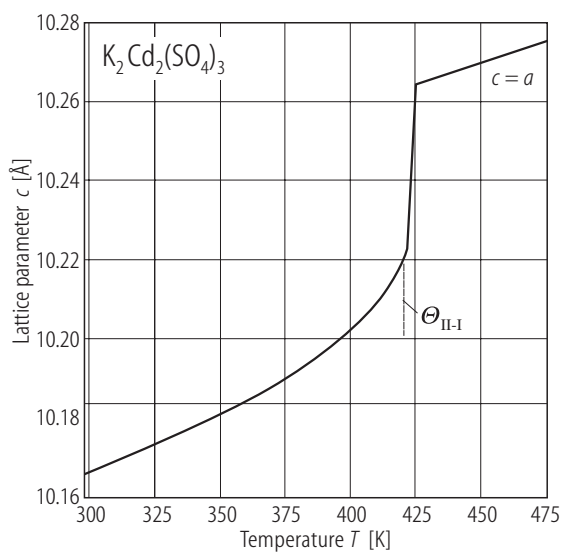


**Fig. 43A-12-007.**  $\text{K}_2\text{Cd}_2(\text{SO}_4)_3$ .  $c$  vs.  $T$  [79Lis].  $c$ : lattice constant measured by dilatometric expansion measurement. The value at 298 K is taken from [77Abr].

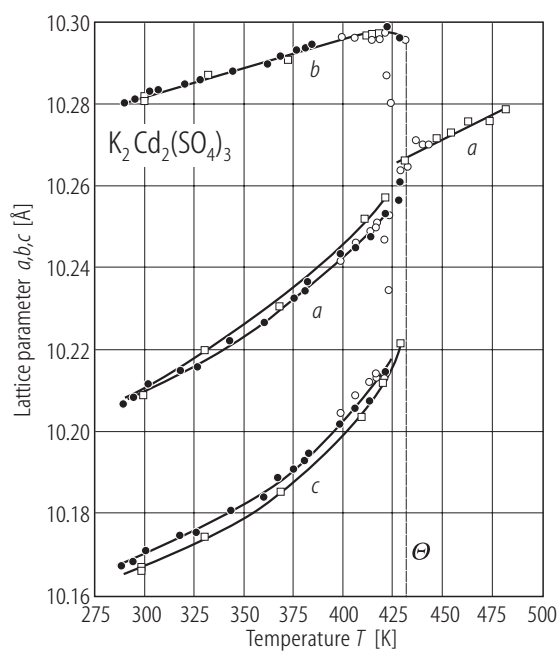


**Fig. 43A-12-008.**  $\text{K}_2\text{Cd}_2(\text{SO}_4)_3$ .  $a$ ,  $b$ ,  $c$  vs.  $T$  [79Lis].  $a$ ,  $b$ ,  $c$ : lattice constants measured by X-ray diffraction. Full circle: the first crystal on heating; open circle: the first crystal on cooling; open square: the second crystal on heating.

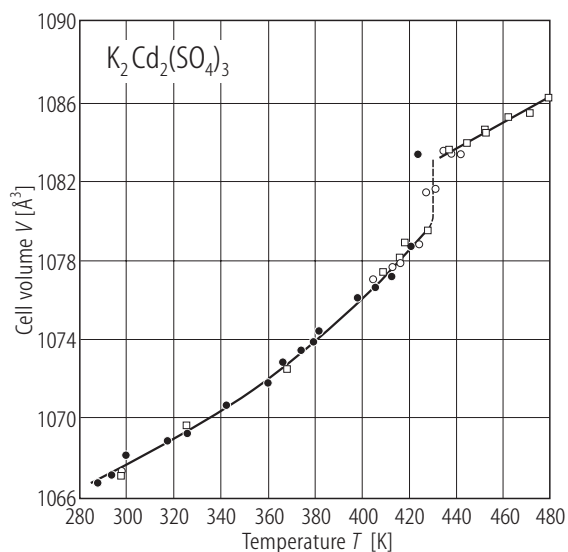


**Fig. 43A-12-009.**  $\text{K}_2\text{Cd}_2(\text{SO}_4)_3$ .  $V$  vs.  $T$  [79Lis].  $V$ : unit cell volume measured by X-ray diffraction. Full circle: the first crystal on heating; open circle: the first crystal on cooling; open square: the second crystal on heating.

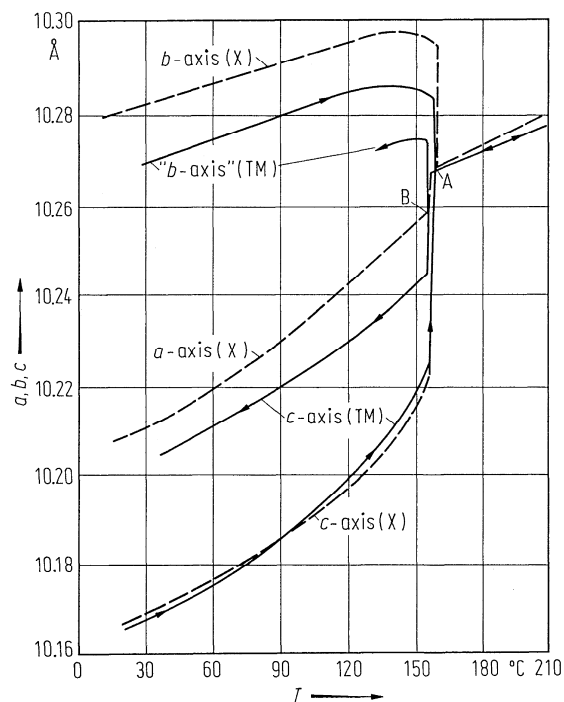


**Fig. 43A-12-010.**  $\text{K}_2\text{Cd}_2(\text{SO}_4)_3$ . Unit cell parameters vs.  $T$  [77Nas]. Full curves (TM): thermal expansion data. Broken curves (X): X-ray diffraction data after [79Lis]. Superposed at point A. On cooling there was an initial contraction of 0.147% from A to B.

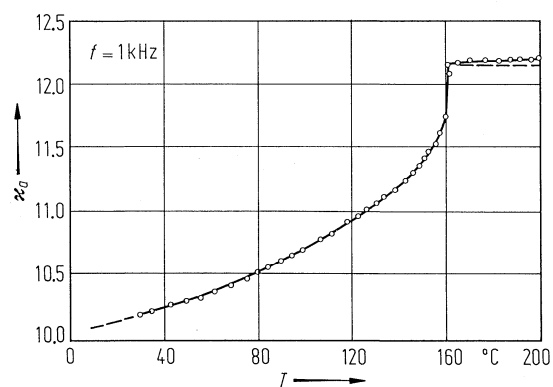


**Fig. 43A-12-011.**  $\text{K}_2\text{Cd}_2(\text{SO}_4)_3$ .  $\kappa_a$  vs.  $T$  [82Poz].  $f = 1 \text{ kHz}$ .

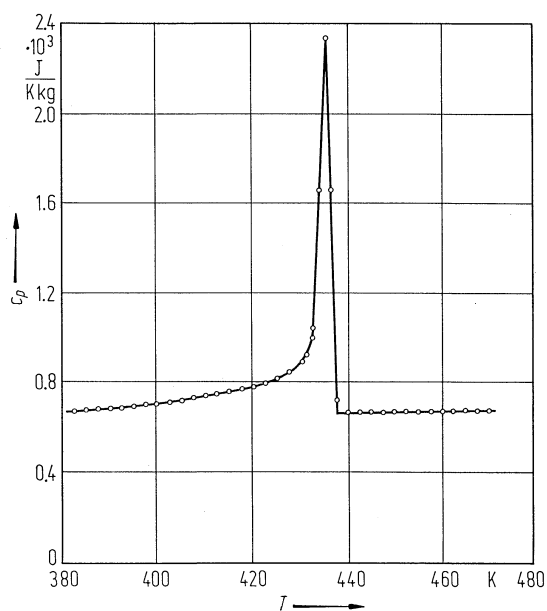


**Fig. 43A-12-012.**  $\text{K}_2\text{Cd}_2(\text{SO}_4)_3$ .  $c_p$  vs.  $T$  [84Dev].  $c_p$ : specific heat capacity at constant pressure.

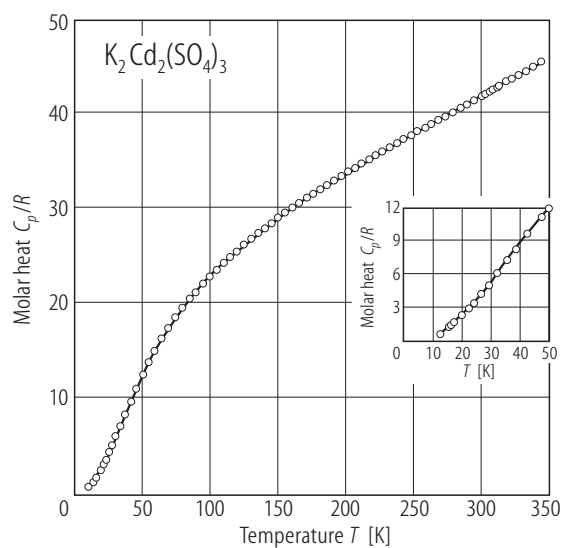


**Fig. 43A-12-013.**  $\text{K}_2\text{Cd}_2(\text{SO}_4)_3$ .  $C_p/R$  vs.  $T$  [94Cao].  $C_p$ : molar specific capacity at constant pressure.

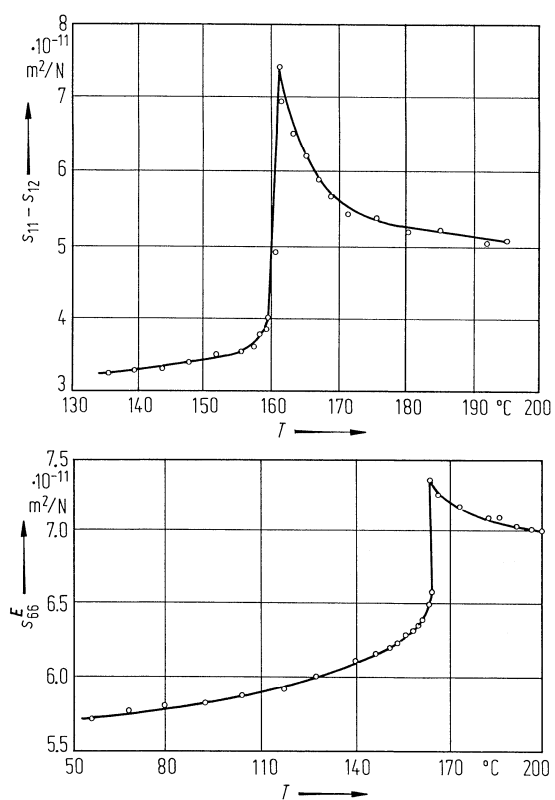


**Fig. 43A-12-014.**  $\text{K}_2\text{Cd}_2(\text{SO}_4)_3$ .  $s_{11} - s_{12}$ ,  $s_{66}^E$  vs.  $T$  [81Ant].



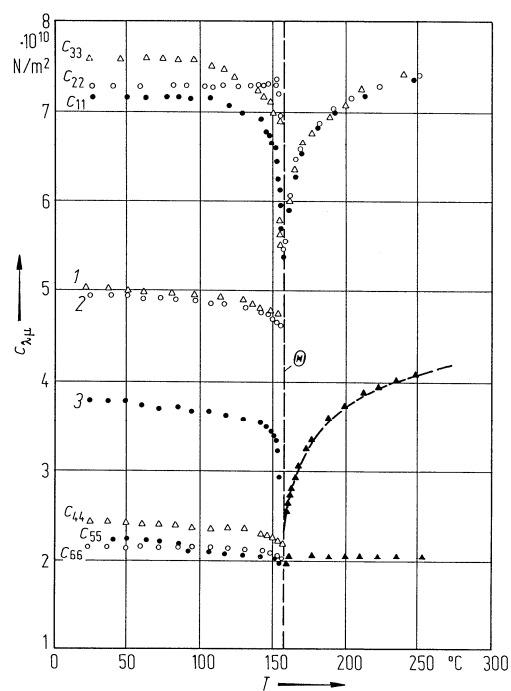


**Fig. 43A-12-015.**  $\text{K}_2\text{Cd}_2(\text{SO}_4)_3$ .  $c_{\lambda\mu}$  vs.  $T$  [83Ant]. Measured by ultrasonic method.  $f = 10$  MHz. 1:  $q \parallel [110]$ ,  $u \parallel [1\bar{1}0]$ ; 2:  $q \parallel [101]$ ,  $u \parallel [10\bar{1}]$ ; 3:  $q \parallel [011]$ ,  $u \parallel [0\bar{1}1]$ .  $u$ : polarization (displacement) vector,  $q$ : wave vector.

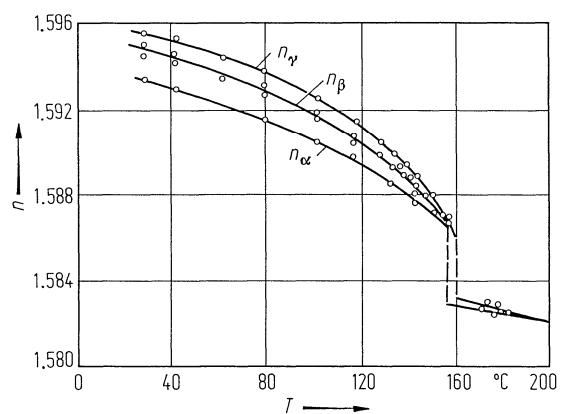


**Fig. 43A-12-016.**  $\text{K}_2\text{Cd}_2(\text{SO}_4)_3$ .  $n$  vs.  $T$  [84Ber].  $\lambda = 546$  nm.  $n_{\alpha}$ ,  $n_{\beta}$ ,  $n_{\gamma}$ : principal refractive indices.

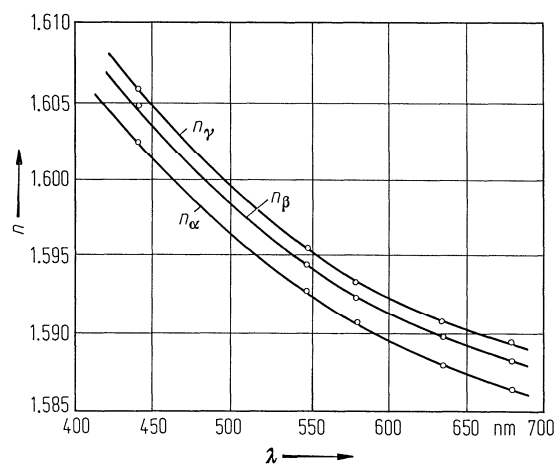


**Fig. 43A-12-017.**  $\text{K}_2\text{Cd}_2(\text{SO}_4)_3$ .  $n$  vs.  $\lambda$  [84Ber].  $T = \text{RT}$ .  $n_\alpha$ ,  $n_\beta$ ,  $n_\gamma$ : principal refractive indices.

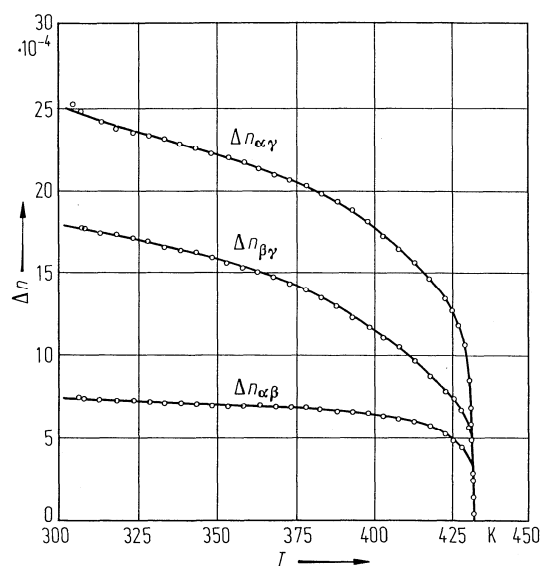


**Fig. 43A-12-018.**  $\text{K}_2\text{Cd}_2(\text{SO}_4)_3$ .  $\Delta n$  vs.  $T$  [84Dev].  $\lambda = 632.8 \text{ nm}$ .

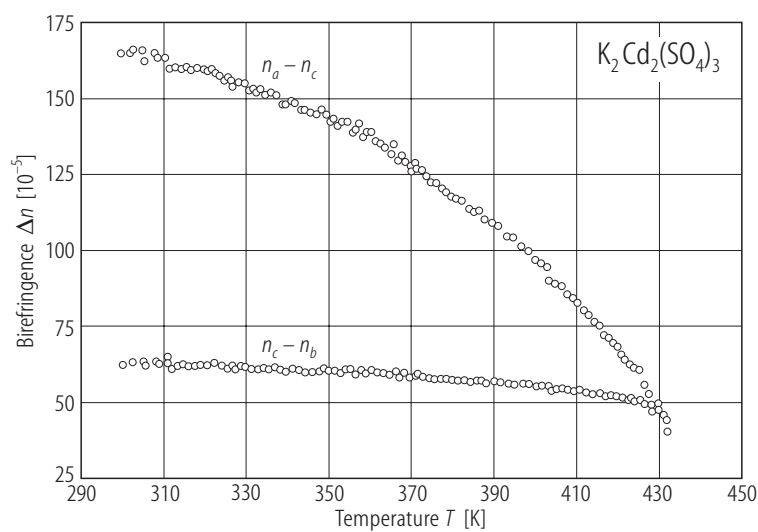


**Fig. 43A-12-019.**  $\text{K}_2\text{Cd}_2(\text{SO}_4)_3$ .  $(n_a - n_c)$  and  $(n_c - n_b)$  vs.  $T$  [96Kam].  $\lambda = 680$  nm.

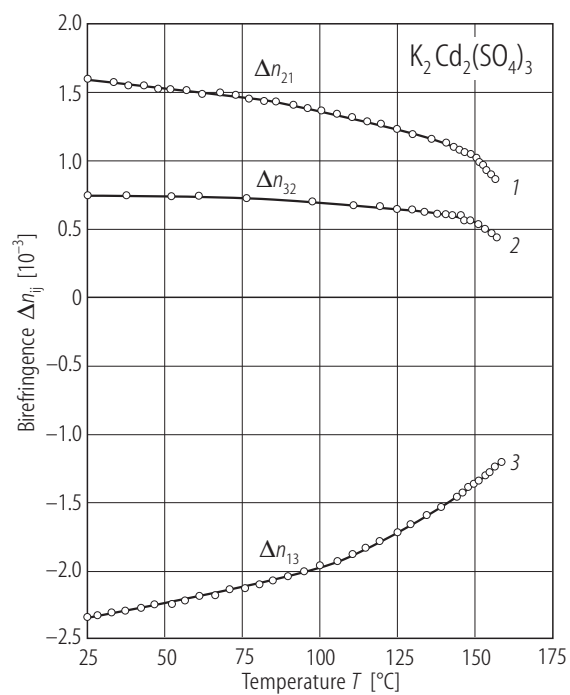


**Fig. 43A-12-020.**  $\text{K}_2\text{Cd}_2(\text{SO}_4)_3$ .  $\Delta n_{21}$ ,  $\Delta n_{32}$ ,  $\Delta n_{13}$  vs.  $T$  [88Bil].  $\lambda = 632.8$  nm.

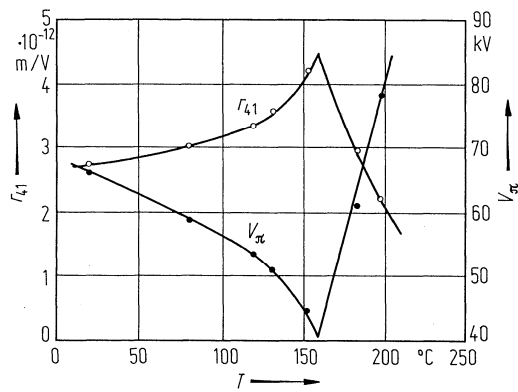


Fig. 43A-12-021.  $\text{K}_2\text{Cd}_2(\text{SO}_4)_3$ .  $r_{41}$ ,  $V_\pi$  vs.  $T$  [84Vlo].  $\lambda = 546 \text{ nm}$ .

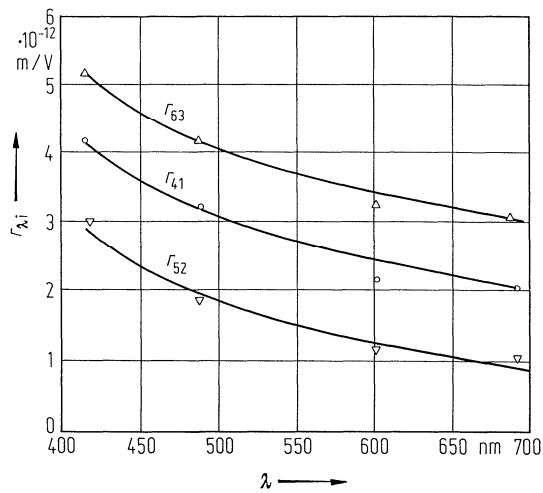


Fig. 43A-12-022.  $\text{K}_2\text{Cd}_2(\text{SO}_4)_3$ .  $r_{\lambda i}$  vs.  $\lambda$  [86Vlo].  $T = \text{RT}$ .

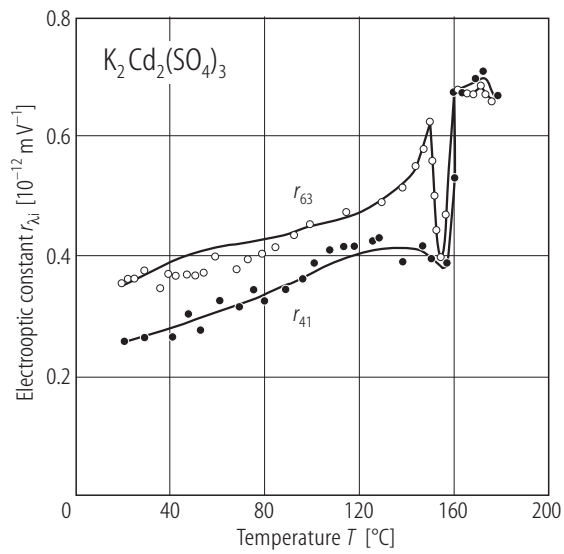
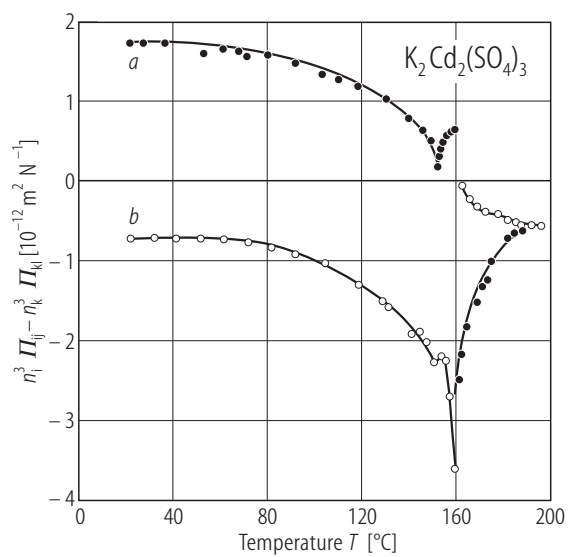
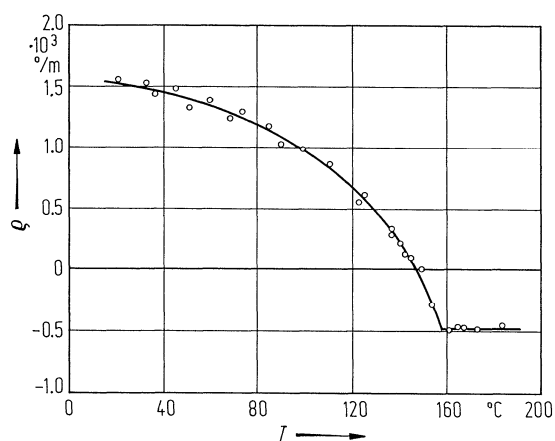


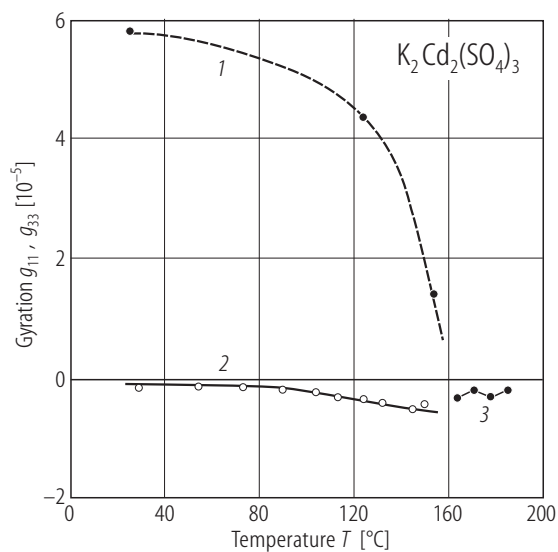
Fig. 43A-12-023.  $\text{K}_2\text{Cd}_2(\text{SO}_4)_3$ .  $r_{63}$ ,  $r_{41}$  vs.  $T$  [87Vlo].



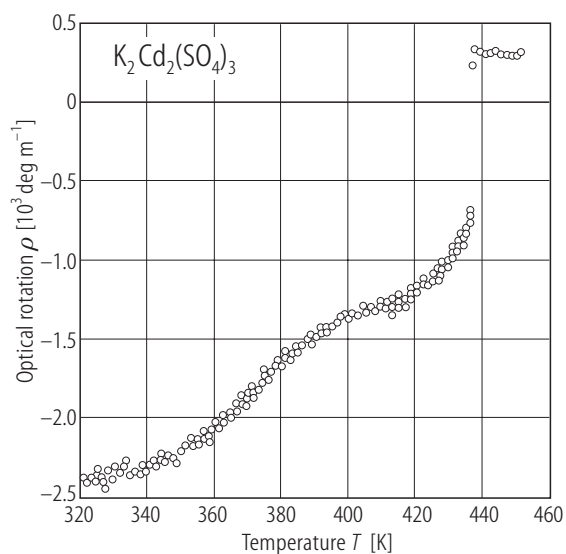
**Fig. 43A-12-024.**  $\text{K}_2\text{Cd}_2(\text{SO}_4)_3$ .  $n_3^3 \Pi_{33} - n_2^3 \Pi_{23}$ ,  $n_1^3 \Pi_{13} - n_3^3 \Pi_{33}$  vs.  $T$  [88Bil]. Curve *a*:  $n_3^3 \Pi_{33} - n_2^3 \Pi_{23}$ ; curve *b*:  $n_1^3 \Pi_{13} - n_3^3 \Pi_{33}$ .  $\lambda = 632.8 \text{ nm}$ .



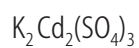
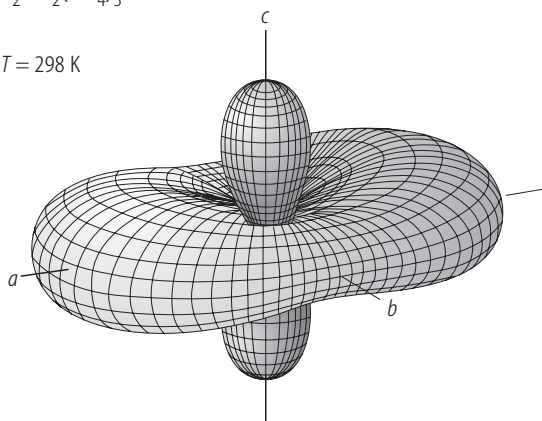
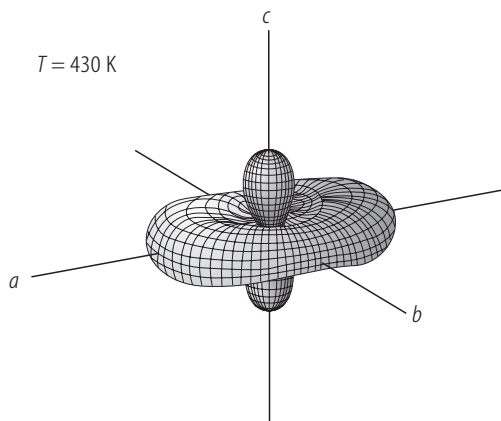
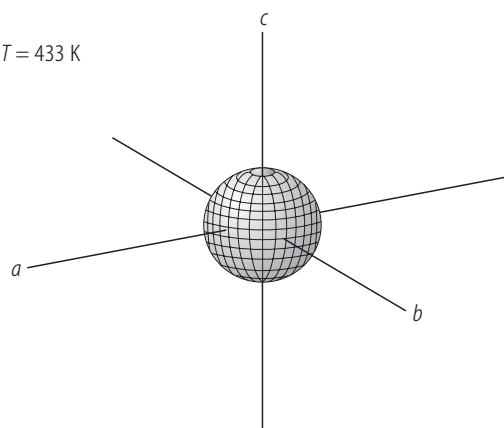
**Fig. 43A-12-025.**  $\text{K}_2\text{Cd}_2(\text{SO}_4)_3$ .  $\rho$  vs.  $T$  [84Vlo].  $\rho$ : optical rotatory power.  $\lambda = 546 \text{ nm}$ .



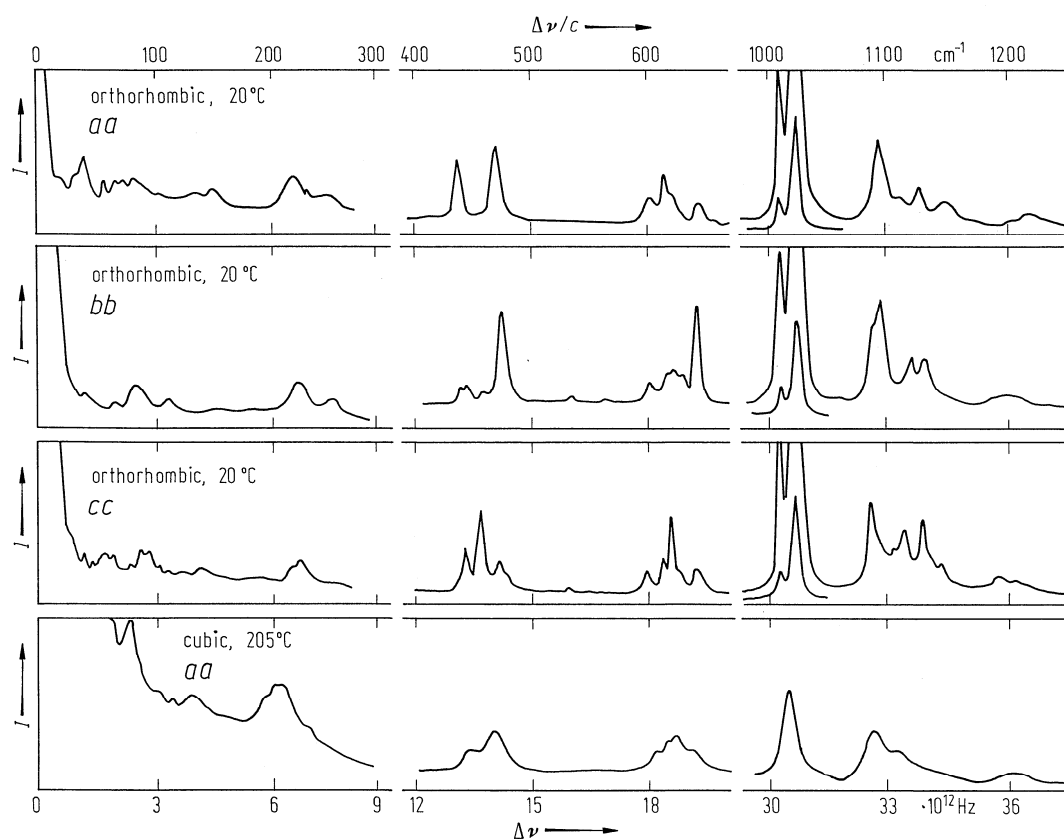
**Fig. 43A-12-026.**  $\text{K}_2\text{Cd}_2(\text{SO}_4)_3$ .  $g_{11}$ ,  $g_{33}$  vs.  $T$  [89Vlo].  $g_{ii}$ : principal value of optical gyration tensor.  $\lambda = 632.8$  nm. 1:  $g_{33}$  in phase II; 2:  $g_{11}$  in phase II; 3:  $g_{11}$  in phase I.



**Fig. 43A-12-027.**  $\text{K}_2\text{Cd}_2(\text{SO}_4)_3$ .  $\rho$  vs.  $T$  [96Kam].  $\rho$ : optical rotatory power along the optical axes.  $\lambda = 680$  nm.

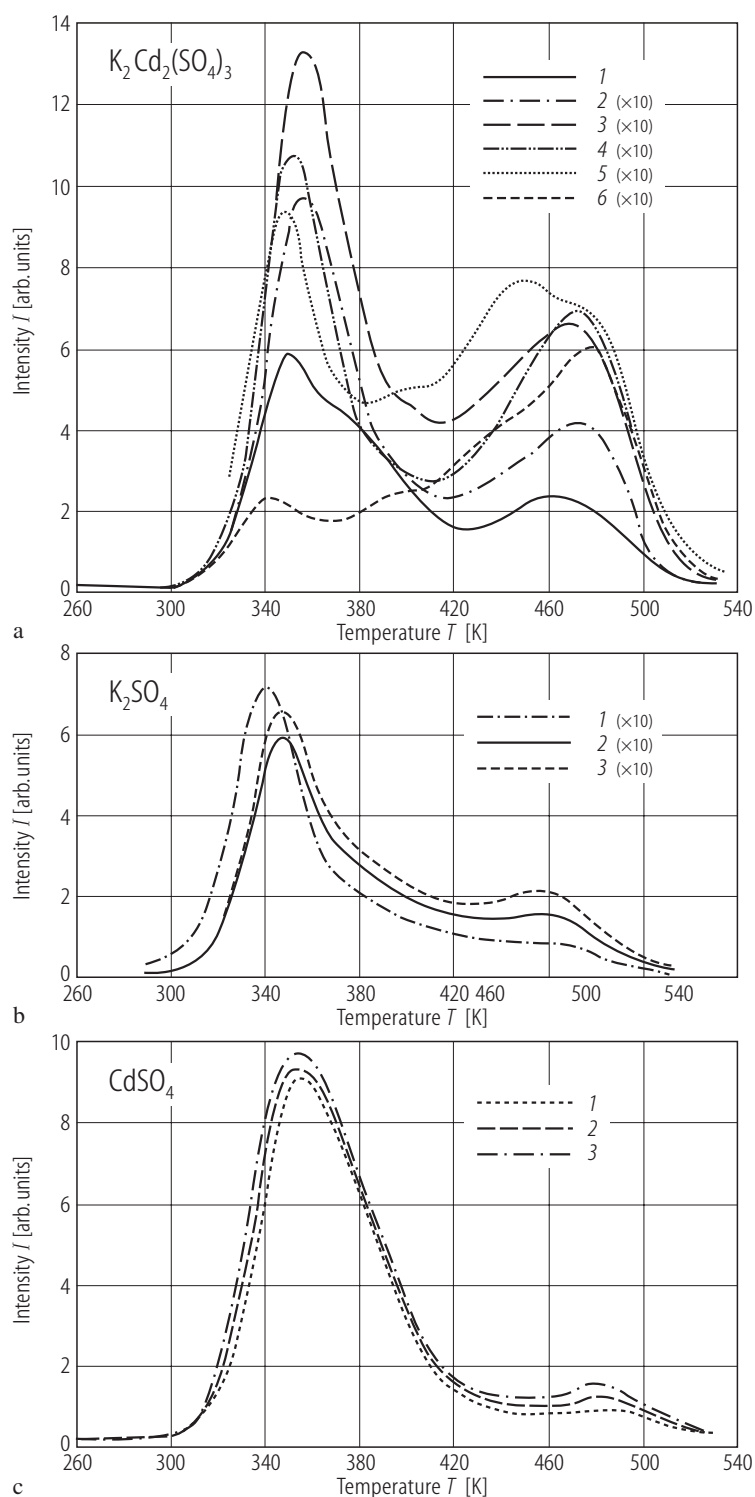

 $T = 298 \text{ K}$ 

 $T = 430 \text{ K}$ 

 $T = 433 \text{ K}$ 


**Fig. 43A-12-028.**  $\text{K}_2\text{Cd}_2(\text{SO}_4)_3$ . Representation surfaces of optical activity for different temperatures [96Kam]. The distance from the origin of the coordinates represents the size of optical activity. Values in cubic phase (433 K) and along  $c$  are positive, values along  $a$  and  $b$  in the orthorhombic phase are negative.



**Fig. 43A-12-029.**  $\text{K}_2\text{Cd}_2(\text{SO}_4)_3$ .  $I$  vs.  $\Delta\nu$  [86Dev].  $I$ : Raman scattering intensity.





**Fig. 43A-12-030.**  $\text{K}_2\text{Cd}_2(\text{SO}_4)_3$ .  $I$  vs.  $T$  [86Des].  $I$ : intensity of thermoluminescence. Parameter: dose of  $\gamma$ -rays of  $^{60}\text{Co}$  source [ $\text{C kg}^{-1}$ ]. (a) (1) 0.756, (2) 7.56, (3) 34, (4) 91, (5)  $272.4 \cdot 10^2$ , (6)  $11 \cdot 10^3$ , (b) (1) 45.4, (2) 136, (3) 227 for  $\text{K}_2\text{SO}_4$ , (c) (1) 45.4, (2) 136, (3) 227 for  $\text{CdSO}_4$ .

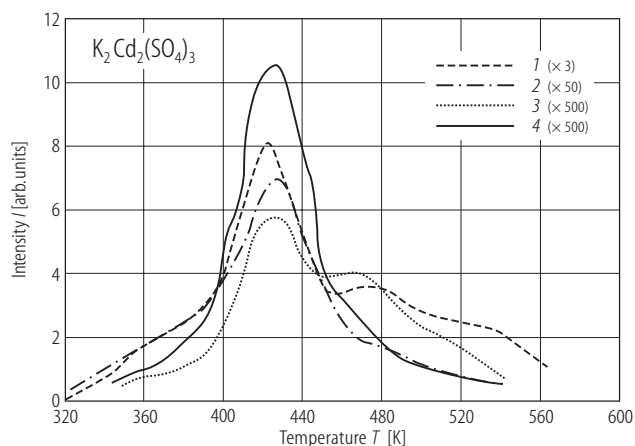


**Fig. 43A-12-031.**  $\text{K}_2\text{Cd}_2(\text{SO}_4)_3$  (0.1% Sm doped).  $I$  vs.  $T$  [86Des].  $I$ : intensity of thermoluminescence. Parameter: dose of  $\gamma$ -rays of  $^{60}\text{Co}$  source [ $\text{C kg}^{-1}$ ]. (1) 0.756, (2) 7.56, (3) 91, (4) 272.4.

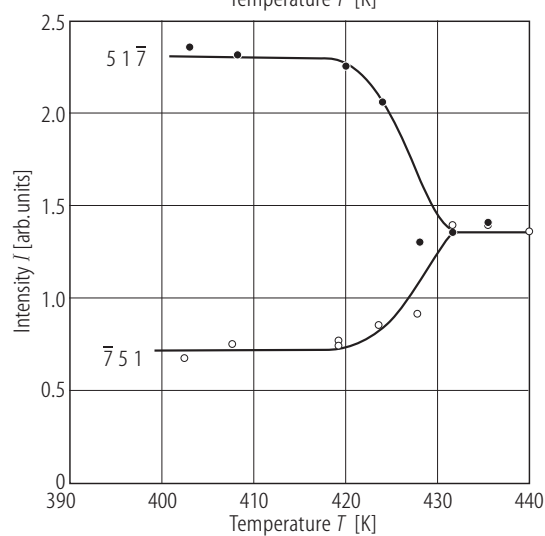
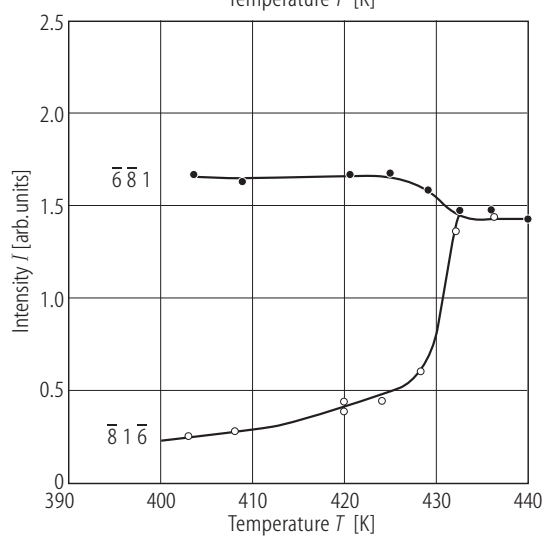
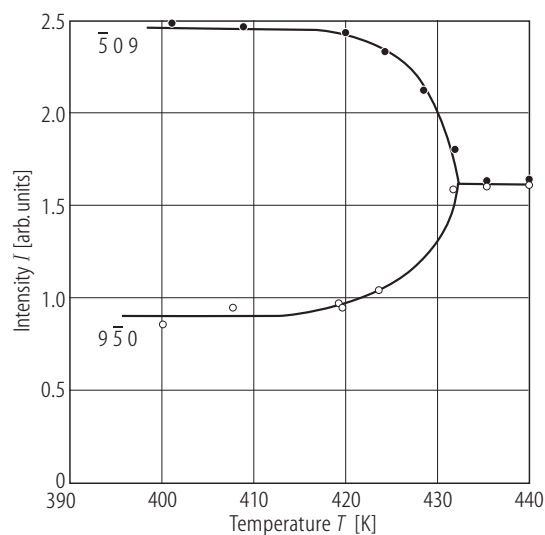
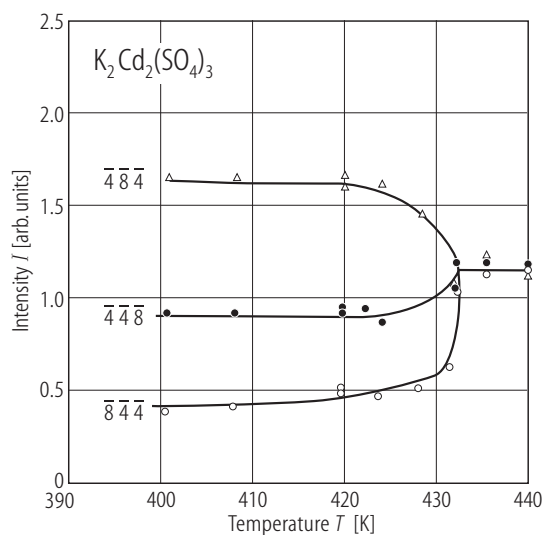


**Fig. 43A-12-032.**  $\text{K}_2\text{Cd}_2(\text{SO}_4)_3$ .  $I$  vs.  $T$  [79Lis].  $I$ : X-ray diffraction intensity.